Observation of local thickness fluctuations in surfactant membranes using neutron spin echo

Michihiro Nagao*

NIST Center for Neutron Research, National Institute of Standards and Technology, Gaithersburg, Maryland 20899-6102, USA and Cyclotron Facility, Indiana University, Bloomington, Indiana 47408-1398, USA

(Received 1 May 2009; revised manuscript received 14 August 2009; published 22 September 2009)

Experimental evidence of local thickness fluctuations of a surfactant membrane, as observed by neutron scattering, is reported. A swollen lamellar structure consisting of nonionic surfactant, water, and oil was investigated by neutron spin echo spectroscopy. Different dynamical processes are recognized at three different length scales. At length scales larger than the membrane thickness, the bending motion is observed, which follows the Zilman and Granek theory [Phys. Rev. Lett. 77, 4788 (1996)]. At the length scale corresponding to the membrane thickness, a clear excess dynamics in addition to the bending motion is observed. This mode is interpreted as the local thickness fluctuations. At even shorter length scales, smaller than the membrane thickness, intramembrane dynamics such as protrusion motions may have been observed.

DOI: 10.1103/PhysRevE.80.031606 PACS number(s): 82.70.Uv, 61.05.fg, 87.16.dj

Surfactant membranes are flexible objects with thermally activated dynamics around room temperatures. The membrane dynamics has been investigated in terms of undulational, peristaltic, and protrusion motions, which originate from the collective movements of the surfactant molecules [1]. These motions appear at different length scales. The undulational motion, which is known to be observed at length scales larger than the membrane thickness, has been well described by the Helfrich bending energy [2], and many experimental investigations have been focused on understanding its properties [3–8]. The peristaltic and the protrusion motions are expected to be observed at length scales shorter than the membrane thickness. However, these dynamics are difficult to investigate experimentally since the membrane thickness is too small to be accessed by techniques using visible light, which typically have been employed for the study of such systems. So far, these membrane motions have been discussed only theoretically [9,10]. The membrane dynamics is particularly interesting for the fluid mosaic model of biomembranes, complex systems consisting of lipids, cholesterol, membrane proteins, etc., which are believed to have, *in vivo*, a complex dynamics relevant for their biological functionality. In this paper, we show evidence that the local thickness fluctuations, which includes peristaltic motion, can be observed by neutron spin echo (NSE) spectroscopy. The present study has exploited the ability of NSE to probe dynamics at length scales from several Å to hundreds Å and time scales ranging from a few ps to hundreds ns [11], which is suitable to observe membrane dynamics.

The bending motion of a surfactant layer has been modeled as a thermally fluctuating thin elastic sheet. Theories based on the Helfrich bending Hamiltonian [2] successfully explained experimental observations in surfactant systems. The steric repulsion between neighboring membranes originates from thermal undulations. At long length scales, the van der Waals attraction and the undulational steric repulsion are the main forces stabilizing the noncharged membrane structure. At shorter length scales, on the order of the membrane thickness, finite thickness and intramembrane structure and dynamics have dominant effects. At this length scale, peristaltic motion, a local thickness fluctuation, takes place [14]. At even shorter length scales, strong short-range repulsion results in a process, in which one or several surfactant molecules protrude from the membrane [12,13]. Recently, the bending, peristaltic, and protrusion motions were observed using molecular dynamics simulation, and in some cases proteins have been included within the membranes to study how the dynamics of the system is affected [9,15,16]. These motions have been modeled theoretically but the results are still under debate because of the lack of experimental observations.

In this paper, we report experimental results of small-angle neutron scattering (SANS) used to characterize the system, and NSE to study the membrane dynamics on a swollen lamellar structure composed of pentaethylene glycol dodecyl ether ($C_{12}E_5$), deuterium oxide (D_2O), and deuterated octane (C_8D_{18}) [17]. The volume fractions of $C_{12}E_5$, D_2O, and C_8D_{18} were $\phi_s=0.041$, $\phi_w=0.9385$, and $\phi_o=0.0205$, respectively. Here, the ratio $\phi_o/\phi_s=0.5$ is used to characterize the system. This sample contained small amount of oil, so that the $C_{12}E_5$ bilayers were slightly swollen by oil and dispersed in D_2O. The temperature was kept at 30 °C for SANS and 29 °C for NSE with a temperature accuracy of ±0.1 °C. At both these temperature the system is in the lamellar phase, and therefore, the 1 °C difference is not relevant. The SANS experiment was conducted on the NG3–30 m SANS at the National Institute of Standards and Technology (NIST) Center for Neutron Research (NCNR) [18]. The incident neutron wavelength λ was selected to be 6 Å with a wavelength spread of 11%. The covered wave vector transfer $q=\frac{4\pi}{\lambda}\sin\theta$ (2θ being the scattering angle) ranged from 0.003 $Å^{-1}$ to 0.3 $Å^{-1}$. The measured two-dimensional data were corrected by the blocked beam and empty cell profiles, azimuthally averaged, and normalized to absolute intensity [19]. The NSE experiment was performed using the NG5-NSE at the NCNR [20,21]. The incident λs were 6 Å and 8.5 Å, and the covered q and time t ranges were $0.038\ Å^{-1}\leq q\leq 0.21\ Å^{-1}$ and $0.05\ \text{ns}\leq t\leq 40$ ns, respectively. The NSE data were normalized by the polarization of

*mnagao@indiana.edu

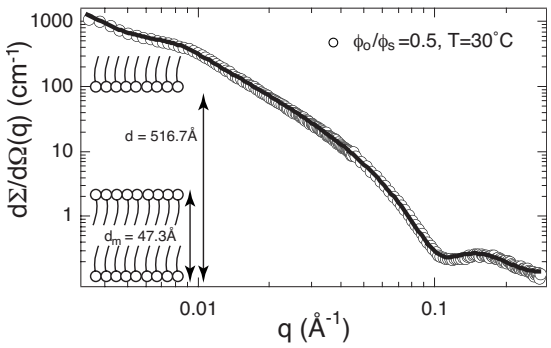

FIG. 1. Observed SANS profile from the sample $\phi_o/\phi_s=0.5$ at $T=30$ °C. The solid line indicates the fit result according to the Lemmich model [23]. The schematic illustration indicates the structure of the swollen lamellar phase. Error bars shown as ±1 standard deviation are smaller than the symbols.

the neutron beam. Carbon powder was used as a standard elastic scatterer to determine the instrumental resolution. The contribution from the solvent scattering was subtracted. These data reductions were performed using the DAVE software [22].

Figure 1 shows a SANS profile for the system at $T=30$ °C. At $q\approx0.009$ Å^{-1}, a correlation peak due to the stacking of the lamellae is observed, and scattering from the form factor of the swollen lamellar membranes appears around $q=0.15$ Å^{-1}. Since isotropic scattering intensities were obtained in the two-dimensional SANS pattern, we treated the present data as the scattering intensity from a powder averaged lamellar structure. This characteristic feature is reproduced using a model scattering function proposed by Lemmich and co-workers for lipid bilayer systems [23]. In the present system, we considered the scattering intensity coming from the layers of surfactant and oil instead of the head and tail layers of lipid molecules in their model. The solid line in Fig. 1 indicates the fit result to the model. The membrane thickness was estimated as $d_m=(47.3\pm14.6)$ Å. Hereafter, we call "membrane" the two surfactant monolayers with the oil layer in between, which is characterized by the scattering intensity at $q>0.1$ Å^{-1} originating from the form factor. The membrane thickness in this case can be calculated from the composition of the sample. For the present composition, $d_m=2(1+\phi_o/\phi_s)d_s$ should be satisfied, where d_s is the length of the surfactant molecule. Assuming $d_s=15.5$ Å [24], $d_m=46.5$ Å is obtained, which is in excellent agreement with the SANS result.

Figure 2(a) shows the normalized intermediate scattering function $I(q,t)/I(q,0)$ observed by NSE. A single membrane dynamics model was proposed by Zilman and Granek [25] for the bending motion, and it has been used to explain the NSE results [26]. Their expression for $I(q,t)/I(q,0)$ is as follows:

$$\frac{I(q,t)}{I(q,0)}=\exp[-(\Gamma t)^{\beta}], \tag{1}$$

where Γ and β are the decay rate and the stretching exponent, respectively. In the case of two-dimensional membranes, $\beta=2/3$ and Γ_{ZG} is proportional to q^3. Γ_{ZG} relates to

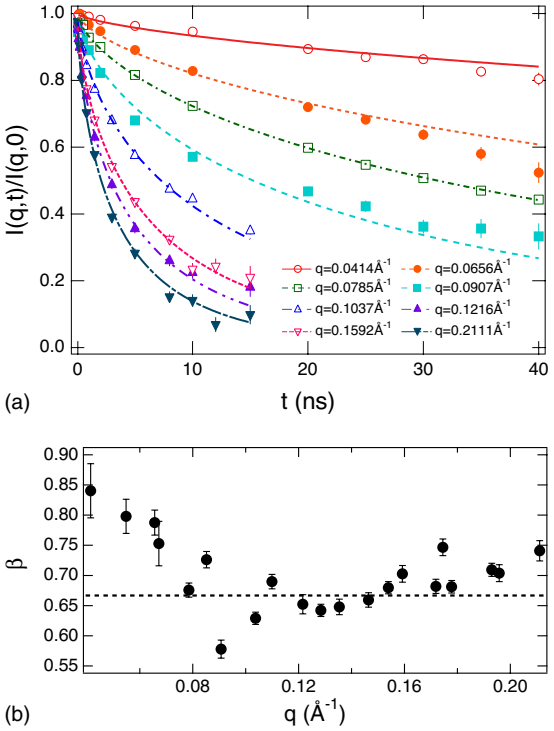

FIG. 2. (Color online) (a) Intermediate scattering function $I(q,t)/I(q,0)$ for $\phi_o/\phi_s=0.5$ at $T=29$ °C. The lines are fit result according to the stretched exponential function with the stretching exponent of 2/3. (b) q dependence of the stretching exponent β when it is a free fit parameter. The dashed horizontal line shows the value $\beta=2/3$. The deviations of β from $\beta=2/3$ in the low-q region could originate from the experimental resolution limit and/or the violation of the Zilman and Granek theory [25] in the long time region.

the bending modulus, κ, of the membrane as,

$$\Gamma_{ZG}=0.025\gamma\left(\frac{k_BT}{\kappa}\right)^{1/2}\left(\frac{k_BT}{\eta}\right)q^3. \tag{2}$$

Where γ originates from averaging over the angle between the wave vector and the plaquette surface normal in the calculation of $I(q,t)/I(q,0)$, k_BT is the thermal energy, and η the solvent viscosity, respectively. Figure 2(b) shows the evaluated q dependence of β, which is scattered around $\beta=2/3$. In the following analyses, we fixed the value of $\beta=2/3$. The lines in Fig. 2(a) are fit results according to Eq. (1) with $\beta=2/3$.

Figure 3 shows the q dependence of the decay rate Γ together with the SANS profile shown in Fig. 1. The solid straight line indicates the q^3 dependence corresponds to the single membrane fluctuation model. As it has been discussed in literature, the membrane shows the bending motion at length scales larger than the membrane thickness [27]. In the low-q region, $\Gamma\propto q^3$ is observed, and it is the evidence for the observation of the bending motion of the surfactant membranes. On the other hand, a clear deviation from the q^3 dependence is observed from $q\approx0.06$ Å^{-1} to $q\approx0.18$ Å^{-1} centered at $q_0\approx0.12$ Å^{-1}. The center, q_0, is close to the dip position in the SANS profile, which indicates that the en-

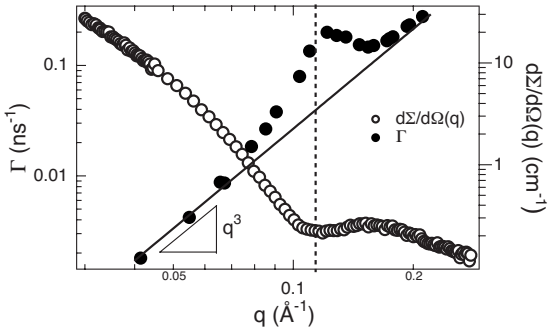

FIG. 3. q dependence of the decay rate Γ for $\phi_o/\phi_s=0.5$ at $T=29$ °C, together with the $d\Sigma/d\Omega(q)$. The solid line shows the q^3 dependence for the Γ axis. The dashed vertical line is the guide for eyes. Error bars are smaller than the symbols.

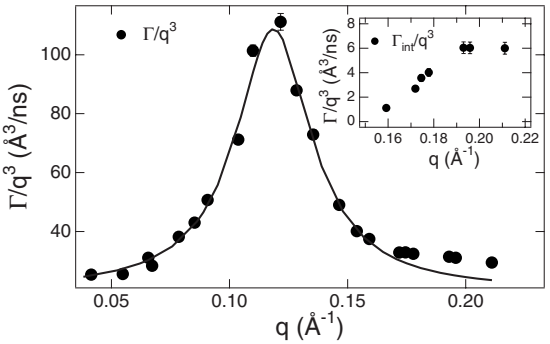

FIG. 4. q dependence of Γ/q^3 for $\phi_o/\phi_s=0.5$ at $T=29$ °C. The solid line is the fit result according to the Lorentz function. The inset figure shows the deviation of the observed data from the fit function at high q, which may indicate the excess intramembrane dynamical modes.

hancement of the dynamics occurs at the length scale corresponding to the membrane thickness. The excess motion is ascribed to the local thickness fluctuations, which include the peristaltic motion of the membrane. An analogy can be drawn between the excess dynamics related to the shape fluctuations of a spherical droplet [4] and the excess dynamics observed in this case.

Schilling and co-workers proposed a theory for the dynamics of the lamellar phase in ternary systems of water, oil, and amphiphile [10]. They treated a bilayer as two combined monolayers, and the mobility degrees of freedom of each monolayer were taken into account. They considered contributions from the bending and the peristaltic motions, and expressed the relaxation rate, ω_s, for such membranes. In the short wavelength limit which is relevant for the present NSE experiment, ω_s for all modes behaves asymptotically as $\omega_s=\kappa q^3/4\eta_{sol}$, where η_{sol} is the averaged solvent viscosity. Even in the longer wavelength cases, their model does not show any peaklike behavior in their dispersion relations, and therefore it cannot explain the present experimental result. To our knowledge, there is no good theory to explain the excess dynamics observed here. However, a recent simulation result by Brannigan and Brown shows a peaklike q dependence in the thickness fluctuation amplitude [16].

In order to investigate the characteristic features of the excess mode dynamics, the q dependence of Γ/q^3 was calculated as shown in Fig. 4. A clear peak profile is obtained, which originates from the excess dynamics in addition to the bending motion of the membrane. In order to discuss deviations from the single membrane fluctuation model, a Lorentz function is utilized to express the local thickness fluctuations as follows:

$$\frac{\Gamma}{q^3}=\frac{\Gamma_{ZG}}{q^3}+\frac{A}{1+(q-q_0)^2\xi^2}, \tag{3}$$

where the first term of the right hand equation accounts for the bending motion, which is explained by the Zilman and Granek theory. The parameters in the Lorentzian relate to the local thickness fluctuations as follows: A can be connected to the damping frequency of the mode, ξ to the mode amplitude, and q_0 is determined by the form factor of the lamellar structure and relates to the membrane thickness. This assignment of the parameters comes from the dimensional analysis and the analogy of the shape fluctuations of droplet microemulsions [28].

The solid line in Fig. 4 indicates the fit result according to Eq. (3). The best fit parameters are $\Gamma_{ZG}/q^3=(19.7\pm0.8)$ Å^3/ns, $A=(89.0\pm1.5)$ Å^3/ns, $q_0=(0.1186\pm0.0002)$ Å^{-1}, and $\xi=(51.3\pm1.6)$ Å, respectively. The term Aq_0^3 corresponds to the decay rate of the local thickness fluctuations. From our fits, $Aq_0^3=(1.48\pm0.03)\times10^8$ s^{-1}, which decreases with temperature [29] and is close to the decay rate of the shape fluctuation motion in pentaethylene glycol decyl ether ($C_{10}E_5$), water, and octane droplet microemulsion [5]. This result suggests that the local thickness fluctuations in the swollen lamellar phase yield the shape fluctuations in the droplet phase, which exists in the lower-temperature region.

Employing Eq. (2), we obtained the value of $\kappa=(1.04\pm0.04)\times10^{-20}$ J$=(2.6\pm0.1)k_BT$. It is known that the Zilman and Granek theory fails to explain the absolute value of κ. In order to avoid this problem, Mihailescu *et al.* proposed the integration analyses for the model [30]. In contrast to this treatment, an empirical rule is to take into account the energy dissipation around the membranes by increasing the effective solvent viscosity by a factor of 3 [31]. Here, we used the latter method to deduce κ using an effective viscosity of $3\eta_{D_2O}$ and $\gamma=1$ in Eq. (2), which is the same treatment for estimating κ of the $C_{12}E_5$ monolayers used by Takeda *et al.* [26]. Although the absolute value of κ cannot be determined with confidence by this treatment, it is generally accepted that relative changes in κ are measured correctly. The present value of κ is about twice of $C_{12}E_5$ monolayers [26]. Probably, the estimated bending modulus is that of the bilayers. The membrane is swollen by oil, but still the synchronization of two monolayers behaves somehow like bilayers. Actually, Freyssingeast *et al.* [32] and Kurtisovski *et al.* [33] showed a decrease of κ with increasing membrane thickness, which are swollen by a small amount of water.

Finally, we would like to discuss the deviation of the observed Γ/q^3 from the Lorentz function as the difference between those, Γ_{int}/q^3, in the high-q range. The inset of Fig. 4 shows the q dependence of Γ_{int}/q^3. An increase of the Γ_{int}/q^3 is observed in the high-q range. Although the meaning of the

Lorentz function is not clear, the deviation from both the Zilman and Granek theory and the Lorentz function might give us a slight hint for some other intramembrane dynamics in the shorter length scales than the membrane thickness. One typical example of such a mode is the protrusion motion of the surfactant molecules at the surface of the membrane [12,13].

In summary, we have investigated the membrane dynamics of a swollen lamellar phase. The surfactant bilayers are swollen by a small amount of oil, and local thickness fluctuations are observed. The q dependence of the relaxation rate of the local thickness fluctuations is reproduced using a Lorentz function, and the relations between fit and dynamical mode parameters are assigned. At the length scale around the membrane thickness, the bending, local thickness fluctuation, and perhaps protrusion motions are observable by the NSE technique. It would be also possible to observe these modes in lipid vesicles containing membrane proteins and/or cholesterol. These investigations will improve the current understandings of the membrane dynamics, which have been investigated mainly by simulations so far.

The author acknowledges A. Faraone for his critical reading of the paper, D. Neumann, and H. Seto for discussions, and P. Butler and S. R. Kline for their help in performing the SANS experiment. This work utilized facilities supported in part by the National Science Foundation under Agreement No. DMR-0454672.

[1] S. A. Safran, *Statistical Thermodynamics of Surfaces, Interfaces, and Membranes* (Addison-Wesley, Reading, MA, 1994).
[2] W. Helfrich, Z. Naturforsch. C **28**, 693 (1973).
[3] F. Nallet, D. Roux, and J. Prost, J. Phys. (France) **50**, 3147 (1989).
[4] B. Farago, D. Richter, J. S. Huang, S. A. Safran, and S. T. Milner, Phys. Rev. Lett. **65**, 3348 (1990).
[5] T. Hellweg and D. Langevin, Phys. Rev. E **57**, 6825 (1998).
[6] C.-H. Lee, W.-C. Lin, and J. Wang, Phys. Rev. E **64**, 020901(R) (2001).
[7] M. Nagao and H. Seto, Phys. Rev. E **78**, 011507 (2008).
[8] Z. Yi, M. Nagao, and D. P. Bossev, J. Phys.: Condens. Matter **21**, 155104 (2009).
[9] E. Lindahl and O. Edholm, Biophys. J. **79**, 426 (2000).
[10] T. Schilling, O. Theissen, and G. Gompper, Eur. Phys. J. E **4**, 103 (2001).
[11] F. Mezei, Z. Phys. **255**, 146 (1972).
[12] J. N. Israelachvili and H. Wennerström, Langmuir **6**, 873 (1990).
[13] R. Lipowsky and S. Grotehans, EPL **23**, 599 (1993).
[14] J. N. Israelachvili and H. Wennerström, J. Phys. Chem. **96**, 520 (1992).
[15] N. Gov, Phys. Rev. Lett. **93**, 268104 (2004).
[16] G. Brannigan and F. L. H. Brown, Biophys. J. **90**, 1501 (2006).
[17] R. Strey, J. Wlakler, and L. Magid, J. Phys. Chem. **95**, 7502 (1991).
[18] C. J. Glinka, J. G. Barker, B. Hammouda, S. Krueger, J. J. Moyer, and W. J. Orts, J. Appl. Crystallogr. **31**, 430 (1998).
[19] S. R. Kline, J. Appl. Crystallogr. **39**, 895 (2006).
[20] N. Rosov, S. Rathgeber, and M. Monkenbusch, in *Scattering from Polymers: Characterization by X-rays, Neutrons, and Light*, edited by P. Cebe, B. S. Hsaio, and D. J. Lohse, ACS Symposium Series No. 739 (American Chemical Society, Washington D. C., 2000), p. 103.
[21] M. Monkenbusch, R. Schätzler, and D. Richter, Nucl. Instrum. Methods Phys. Res. A **399**, 301 (1997).
[22] http://www.ncnr.nist.gov/dave/
[23] J. Lemmich, K. Mortensen, J. H. Ipsen, T. Hønger, R. Bauer, and O. G. Mouritsen, Phys. Rev. E **53**, 5169 (1996).
[24] M. Nagao, H. Seto, D. Ihara, M. Shibayama, and T. Takeda, J. Chem. Phys. **123**, 054705 (2005).
[25] A. G. Zilman and R. Granek, Phys. Rev. Lett. **77**, 4788 (1996).
[26] T. Takeda, Y. Kawabata, H. Seto, S. Komura, S. K. Ghosh, M. Nagao, and D. Okuhara, J. Phys. Chem. Solids **60**, 1375 (1999).
[27] R. Goetz, G. Gompper, and R. Lipowsky, Phys. Rev. Lett. **82**, 221 (1999).
[28] S. T. Milner and S. A. Safran, Phys. Rev. A **36**, 4371 (1987).
[29] M. Nagao (unpublished).
[30] M. Mihailescu, M. Monkenbusch, H. Endo, G. Gompper, J. Stellbrink, D. Richter, B. Jakobs, T. Sottmann, and B. Farago, J. Chem. Phys. **115**, 9563 (2001).
[31] S. Komura, T. Takeda, Y. Kawabata, S. K. Ghosh, H. Seto, and M. Nagao, Phys. Rev. E **63**, 041402 (2001).
[32] E. Freyssingeas, D. Roux, and F. Nallet, J. Phys.: Condens. Matter **8**, 2801 (1996).
[33] E. Kurtisovski, N. Taulier, R. Ober, M. Waks, and W. Urbach, Phys. Rev. Lett. **98**, 258103 (2007).